© 2018. Published by The Company of Biologists Ltd | Development (2018) 145, dev164111. doi:10.1242/dev.164111

RESEARCH ARTICLE

Differential expression of Öbek controls ploidy in the *Drosophila* blood-brain barrier

Selen Zülbahar[1], Florian Sieglitz[1], Rita Kottmeier[1], Benjamin Altenhein[2], Sebastian Rumpf[1] and Christian Klämbt[1,*]

ABSTRACT

During development, tissue growth is mediated by either cell proliferation or cell growth, coupled with polyploidy. Both strategies are employed by the cell types that make up the *Drosophila* blood-brain barrier. During larval growth, the perineurial glia proliferate, whereas the subperineurial glia expand enormously and become polyploid. Here, we show that the level of ploidy in the subperineurial glia is controlled by the N-terminal asparagine amidohydrolase homolog Öbek, and high Öbek levels are required to limit replication. In contrast, perineurial glia express moderate levels of Öbek, and increased Öbek expression blocks their proliferation. Interestingly, other dividing cells are not affected by alteration of Öbek expression. In glia, Öbek counteracts fibroblast growth factor and Hippo signaling to differentially affect cell growth and number. We propose a mechanism by which growth signals are integrated differentially in a glia-specific manner through different levels of Öbek protein to adjust cell proliferation versus endoreplication in the blood-brain barrier.

KEY WORDS: *Drosophila*, Glia, N-end rule pathway, Blood-brain barrier, Endomitosis, Öbek, NTAN1

INTRODUCTION

During development, regulation of cell size, as well as cell number, is of obvious importance. In the developing nervous system, not only the number of neurons and glial cells needs to be properly adjusted, but also the size of neurons and glial cells needs to be matched to the developmental stage. In this respect, glial and neuronal cell growth must be tightly regulated to ensure that cell size is always well adjusted. Cell size is controlled through a balance of growth and division (Wood and Nurse, 2015). A proportionality between cell size and ploidy is long known but the molecular mechanisms underpinning the control of polyploidy are not well understood (Edgar et al., 2014; Orr-Weaver, 2015).

The peripheral nervous system (PNS) of *Drosophila* larvae harbors sensory neurons projecting their axons towards the brain and motor axons, which project from the central nervous system (CNS) to the periphery. When the larva hatches from the egg case, the length of the longest nerves measures only ∼150 µm (Campos-Ortega, 1997). During the next 3 days, the animal shows an enormous growth, and nerves then reach a length of more than 2500 µm (von Hilchen et al., 2013; Matzat et al., 2015). The peripheral nerves of *Drosophila* are accompanied by a small set of glial cells, consisting of the wrapping glia and glial cells of the blood-brain barrier (Stork et al., 2008). Three wrapping glial cells are found at each of the segmentally organized nerves (von Hilchen et al., 2008, 2013; Sepp et al., 2000). These glial cells are born during mid-embryonic stages and do not proliferate during the entire larval life. Instead, the wrapping glia appear to show a lifelong growth program as they continuously wrap more and more axons as the larva grows (Matzat et al., 2015; Stork et al., 2008).

The blood-brain barrier contains two morphologically distinct cell types: the small perineurial glial cells and the large subperineurial glial cells (SPGs). Only five perineurial glial cells are generated during embryonic stages, one of which (ePG2) is located at the long, stretched part of the nerve, which extends across the different segmental units, also called the nerve extension region (NER). Unlike most other glial cells in abdominal nerves, the ePG2 divides extensively to adjust glial cell number to the increasing length of the segmental nerves (Matzat et al., 2015; von Hilchen et al., 2008, 2013; Silies et al., 2007; Stork et al., 2008). The perineurial glial cells maximize their cell surface through division and generation of many cell processes, possibly to take up the nutrients such as trehalose from the hemolymph (Stork et al., 2008; Volkenhoff et al., 2015).

In contrast to this, the SPGs do not divide. They are born during embryonic stages and have to build up a functional blood-brain barrier before the animal emerges from the egg case (Stork et al., 2008). Only four SPGs are found along each embryonic nerve, one of which is located in the NER (von Hilchen et al., 2008, 2013). SPGs are very large cells that expand and become polyploid during development (Unhavaithaya and Orr-Weaver, 2012). This ensures that the diffusion barrier established by the SPGs stays intact throughout development, which otherwise would be disrupted through cell division. Interestingly, the SPGs are an unusual type of polyploid cell, as both endomitosis as well as endoreplication contribute to their growth (Orr-Weaver, 2015; Unhavaithaya and Orr-Weaver, 2012). Therefore, the two cell types of the blood-brain barrier behave differentially during larval growth: the perineurial glial cells proliferate, whereas the SPGs increase their size and the level of ploidy.

Several models have been put forward to link cell growth and ploidy, some of which propose that changing concentration of an unknown factor might be regulating the decision between ploidy and division (Marshall et al., 2012). The levels of cellular proteins can be regulated through transcriptional control or post-transcriptional modulation of translation efficacy, protein stability and turnover. Protein turnover is mostly regulated through the ubiquitin-proteasome system (Ciechanover, 2005). Here, specific ubiquitin ligases are needed that can be recruited to their substrate

[1]Institute of Neurobiology, University of Münster, Badestrasse 9, 48149 Münster, Germany. [2]Institute of Zoology, University of Cologne, Zülpicher Straße 47b, 50674 Cologne, Germany.

*Author for correspondence (klaembt@uni-muenster.de)

C.K., 0000-0002-6349-5800

Received 6 February 2018; Accepted 3 July 2018

Development (2018) 145, dev164111. doi:10.1242/dev.164111

proteins by manifold regulatory systems (Zheng and Shabek, 2017). One of these systems is the N-end rule pathway, which recognizes proteins carrying destabilizing N-terminal amino acids and subsequently generates ubiquitinated substrates for proteasomal degradation (Bachmair et al., 1986; Sriram et al., 2011).

Here, we report that the gene *öbek* (*CG5473*; *SP2637* – FlyBase), which encodes the *Drosophila* N-terminal asparagine amidohydrolase (NTAN1) homolog acting in the N-end rule pathway, as a regulator of endoreplication rates in SPGs. We detected asparagine amidohydrolase activity of Öbek in glial cells and show that Öbek controls ploidy and the number of nuclei, and hence the extent of endomitosis in SPGs. In these cells, high Öbek levels are of crucial importance to limit cell cycle and replication rates during larval stages. Accordingly, reduced Öbek expression leads to increased ploidy and consequent endomitosis in peripheral SPGs. On the other hand, perineurial glial cells, which express moderate levels of Öbek, are less sensitive to loss of Öbek function, and increased Öbek levels block their proliferation. We also show that Öbek counteracts the activity of Yorkie, a member of the Hippo pathway, as well as the activity of the fibroblast growth factor (FGF) receptor Heartless in glial cells. We propose a mechanism by which different Öbek levels regulate the distinct responses to similar growth cues in different glial cells of the blood-brain barrier.

RESULTS

Identification of the *öbek* gene

To identify novel regulators of glial cell growth, we screened for genes that, when suppressed, lead to glial growth defects resulting in nerve bulges in the abdominal peripheral nerves of *Drosophila*. Such a phenotype could be an indication of either disrupted ion homeostasis or defective glial growth (Ghosh et al., 2013; Leiserson et al., 2000, 2011). In the PNS of *Drosophila*, control third-instar larvae have compacted nerves which are accompanied by glial membranes (green in Fig. 1A-B′) and regularly spaced glial nuclei (Fig. 1A,A′) (von Hilchen et al., 2013; Matzat et al., 2015). Panglial RNA interference (RNAi)-mediated suppression of *CG5473* (*öbek*) results in the appearance of glial nerve bulges accompanied by defasciculated axons (Fig. 1B,B′, arrows) and additional glial nuclei in the NER of the abdominal nerves (Fig. 1B-C). Owing to this knockdown phenotype, which leads to a local accumulation of glial nuclei and increase of total glial nuclei number, we called the gene *öbek* (Turkish for pile or group).

Differential effects of Öbek on peripheral glia

The peripheral nerves harbor three different glial cell types: perineurial, subperineurial and wrapping glia. To test in which glial cell type *öbek* might be acting we performed a subtype-specific knockdown. For wrapping glia-specific knockdown, we utilized the

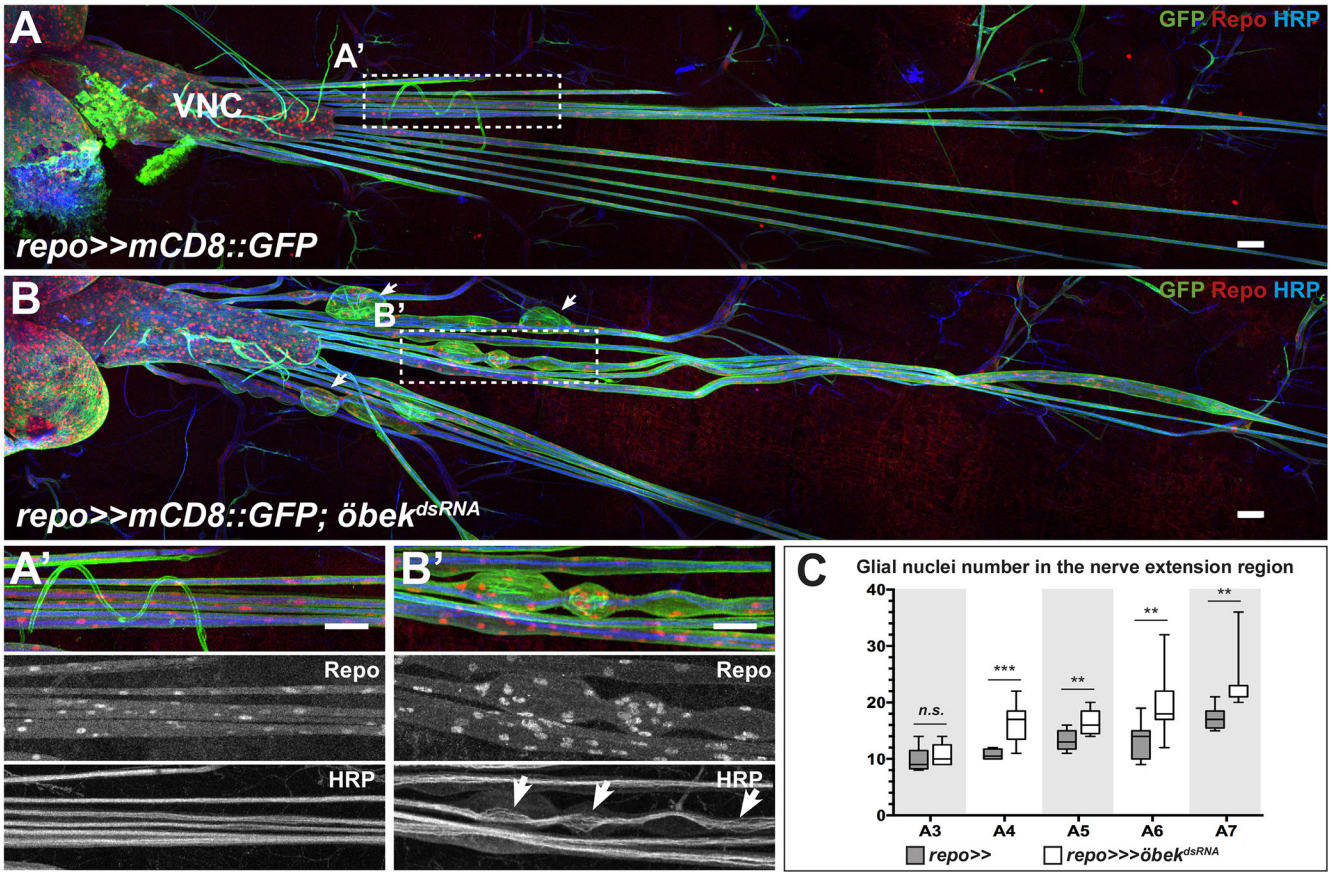

Fig. 1. *öbek* knockdown leads to nerve bulges and increased number of glial nuclei. Representative confocal projections of third-instar larval filet preparations stained as indicated ($n>10$). Glial nuclei are labeled in red (anti-Repo staining), neuronal membranes are shown in blue (anti-HRP staining) and GFP expression is shown in green. (A,A′) In the control animals, each peripheral nerve is enwrapped by glial membranes as detected by *repo>>mCD8::GFP* expression. Glial cell nuclei are evenly distributed along the peripheral nerve tracts (A′) and axons are fasciculated. (B,B′) Panglial knockdown of *öbek* (*CG5473*) leads to bulges along the peripheral nerves. Here, additional glial nuclei are observed and axons defasciculate (arrows in B′). (C) Quantification of the number of glial nuclei along the nerve extension region (NER) of nerves A3-A7. The genotypes are indicated. In all box plots, the box indicates the 50% quartile with the median; whiskers indicate the maximum and the minimum of all the data. $n\geq7$ for each abdominal nerve. n.s., not significant; $^{**}P\leq0.01$, $^{***}P\leq0.001$. Scale bars: 50 µm.

Development (2018) 145, dev164111. doi:10.1242/dev.164111

nrv2-Gal4 driver (Matzat et al., 2015) and observed no axonal defasciculations in the abdominal peripheral nerves or changes in nuclei number of the wrapping glia in these animals (n>5 animals; number of wrapping glial cells in A3-A7, one per NER in wild-type or *nrv2-Gal4>>öbek*^{dsRNA} animals). To test the requirement of *öbek* in the perineurial glia we used the *46F-Gal4* driver (Xie and Auld, 2011). To discriminate the nuclei of different glial subtypes present in the abdominal nerves, we analyzed the expression of the transcription factor Cut, which is strongly expressed in the wrapping glial cells and moderately in the SPGs, and the transcription factor Apontic, which is found in the nuclei of perineurial (strong expression) and SPGs (weak expression) (Bauke et al., 2015; Sasse and Klämbt, 2016). Silencing *öbek* specifically in perineurial glia using the *46F-Gal4* driver does not result in nerve bulges (Fig. 2A,B). However, counting of perineurial glial nuclei revealed a slight increase in nuclei number in the long nerves, A6 and A7 (Fig. 2C; Apontic-positive, Cut-negative nuclei were counted). Next, we silenced *öbek* using the SPG-specific Gal4 drivers *SPG-Gal4* (utilizing enhancer elements of the *moody* gene) or *Gli-Gal4* (*P[Gal4]* insertion in the *Gliotactin* gene) (Schwabe et al., 2005; Sepp and Auld, 1999; Stork et al., 2008). In control animals, in which SPG nuclei were detected by dsRed expression (*Gli>>dsRed*), one to three SPG nuclei per NER were counted, with few exceptions in which we could detect up to seven SPG

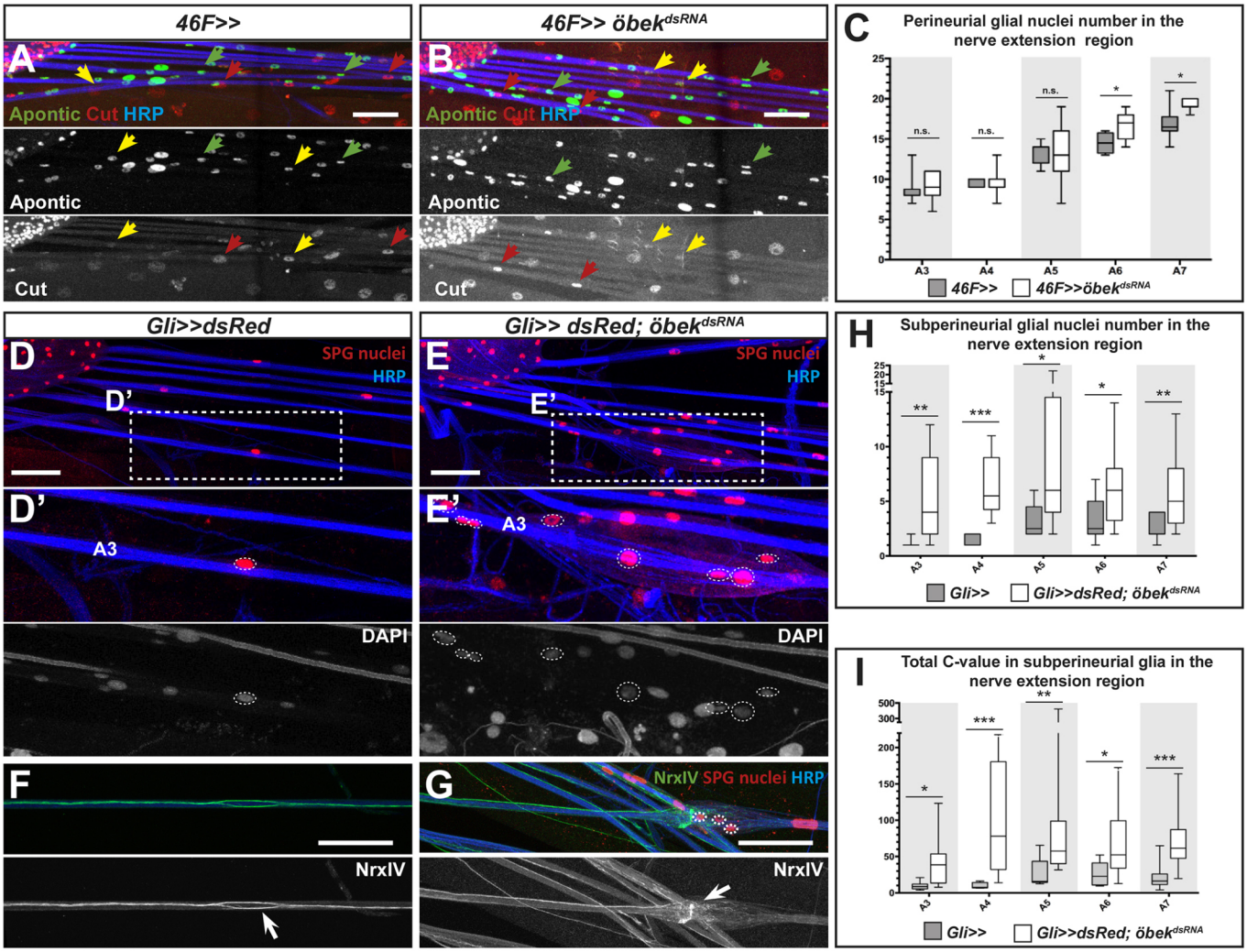

Fig. 2. *öbek* differentially affects replication in peripheral glia. Confocal projections of third-instar larval peripheral nerves stained as indicated. (A,B) Control larva (A) and larva with perineurial glia-specific knockdown of *öbek* using *46F-Gal4* (B). Perineurial glial cells express high levels of Apontic (green arrows). Cut is strongly expressed by wrapping glial cells (red arrows) and weakly expressed by the SPGs, which also express some Apontic (yellow arrows). (C) Perineurial nuclei (Apontic positive and Cut negative) in the different genotypes were counted for each nerve. *öbek* knockdown leads to a slight increase in perineurial glial nuclei number in longer nerves. (D,E) Control larvae (D) and *öbek* knockdown larvae (E) were used to count the SPG nuclei number in the NER (by Gli-Gal4>UAS-StingerRed expression) and to measure the total C-value of the SPG nuclei by DAPI staining. The ventral nerve cord is shown in the top left. The dashed line box indicates the area shown at higher magnification in D′ and E′. (F) Control peripheral nerve, image was taken ∼500 µm posterior to the ventral nerve cord. A line of NrxIV expression highlights the autocellular septate junctions, whereas a ring (arrow) indicates the contact of two neighboring SPGs. Blue, HRP-labeled axons; red, SPG nuclei. (G) Suppression of *öbek* expression in SPGs leads to more nuclei; however, these nuclei are not separated by lines of NrxIV staining (see white dashed line circles; the arrow points towards NrxIV accumulation between two SPGs). Overall, NrxIV expression appears to be increased and disorganized. The image was taken ∼700 µm posterior to the ventral nerve cord. (H) Quantification of the number of SPG nuclei along the NER of nerves A3-A7 as indicated. Number of SPG nuclei per NER increases upon *öbek* knockdown. (I) Quantification of total C-value in SPG nuclei per NER in A3-A7 nerves. The graph shows the sum of the C-values of all the SPG nuclei for every nerve counted. The Mann–Whitney test was applied. The total DNA amount (C-value) increases significantly upon *öbek* knockdown (n≥7 nerves; n.s., not significant; *0.1<P≤0.5; **0.01<P≤0.1; ***0.001<P≤0.01). Scale bars: 50 µm.

Development (2018) 145, dev164111. doi:10.1242/dev.164111

nuclei (Fig. 2D,H). Upon *öbek* knockdown, we observed a significant increase in the number of SPG nuclei with concomitant axonal defasciculation (1-22 nuclei, *n*=56 nerves; Fig. 2E,H).

Interestingly, the first intron of the gene *öbek* is targeted by the *Mz97 P[Gal4]* insertion (herein referred to as *Mz97-Gal4*), which is a well-known marker for SPGs (Beckervordersandforth et al., 2008; von Hilchen et al., 2008; Ito et al., 1995). Moreover, we observed that homozygous *Mz97-Gal4* larvae also show defasciculated segmental nerves with an increased number of *Mz97-Gal4*-positive glial nuclei (Fig. S1A,B, arrows). Instead of isolated *Mz97-Gal4*-positive nuclei as in heterozygous larvae, we observed nerves with clusters of several SPG nuclei and axonal defasciculation (Fig. S1A′,B′, arrows in B′), indicating that *Mz97-Gal4* insertion might have led to a mutant allele for *öbek*. Taken together, these data indicate that Öbek primarily affects nuclei number in the SPGs. In addition, there is a length-dependent effect of *öbek* knockdown on perineurial glia in the abdominal nerves.

Endoreplication rate in the SPGs is controlled by *öbek*

SPGs form during embryonic stages, do not divide during larval development and keep the blood-brain barrier intact. Only one SPG, which is formed during embryogenesis, covers the entire NER during larval stages (von Hilchen et al., 2013). Cellular growth in these cells is accompanied by endoreplication. SPGs of the CNS were shown to be multinucleated, indicating endomitosis in these cells (Unhavaithaya and Orr-Weaver, 2012). Here, we analyzed peripheral SPGs and counted several nuclei in the NER in control animals (Fig. 2H). Interestingly, additional SPG nuclei in the NER were noted also in previous studies (von Hilchen et al., 2013). Therefore, also in the PNS, endomitosis seems to take place in SPGs as has been demonstrated in the CNS (Unhavaithaya and Orr-Weaver, 2012).

To test whether loss of *öbek* triggers cell division in the SPGs, resulting in extra nuclei or rather an increased rate of endomitosis, we stained for NeurexinIV (NrxIV), which is a septate junction marker outlining individual SPGs. A line of NrxIV labels the autocellular septate junctions formed by single SPGs in the PNS, whereas a ring indicates the contact of two different SPGs (Fig. 2F, arrow). Upon *öbek* suppression, we noted increased NrxIV staining, which is not properly organized in a line of septate junctions (Fig. 2G, arrow) and does not separate the extra nuclei, suggesting that the SPGs contain multiple nuclei (Fig. 2G, white dashed line circles outlining the SPG nuclei of a single nerve). Similar conclusions were drawn from stochastic multicolor labeling (MCFO) experiments (Nern et al., 2015). Here, cell-type specific recombination enables labeling of individual cells. As a proof of principle, we induced recombination in the perineurial glia and detected small cells containing a single nucleus labeled in different colors. In contrast, in homozygous *Mz97-Gal4* (*öbek* mutant) larvae, SPGs are large uniformly colored cells and contain many nuclei (Fig. S2).

Next, we measured the total DNA amount (total C-value) of the SPG nuclei per NER through 4′,6-diamidino-2-phenylindole (DAPI) labeling (see Materials and Methods). During larval development, the size of SPGs increases significantly from A1 to A8 nerves to cope with the increasing nerve length in different segments and cover the entire NER (von Hilchen et al., 2013; Matzat et al., 2015). Surprisingly, in control animals, we found no clear correlation between the C-value and nerve length (Fig. 2I, Table S1). In addition to the increase in SPG nuclei number upon *öbek* knockdown, we also noted a pronounced increase in the C-value in all nerves. Several extreme outliers are seen with C-values up to 400 (Fig. 2H,I, Table S1).

We also employed the Fly-FUCCI technique to characterize the cell cycle dynamics of the SPGs, which relies on GFP- or RFP-tagged E2f1 and Cyclin B proteins degraded by the ubiquitin E3-ligases during the onset of S-phase or during mitosis, respectively (Zielke et al., 2014). We observed that S-phase could be more frequently detected in the SPGs of both CNS and PNS upon *öbek* knockdown (Fig. S3).

In conclusion, loss of *öbek* does not trigger cell division but rather causes an increased endoreplication rate and consequently appearance of extra nuclei in the SPGs. Because the DNA content of a cell correlates with its size (Edgar et al., 2014; Orr-Weaver, 2015), we conclude that normal *öbek* function is required to limit DNA replication in SPGs in order to match it to cell growth.

Differential expression of Öbek in peripheral glial cells

To characterize the expression pattern of Öbek, we generated antibodies against a small peptide sequence derived from the deduced Öbek protein (SFPDRGPDRELR, present in all isoforms). Because peripheral glial subtypes are well characterized in the embryo (von Hilchen et al., 2008), we first studied the distribution of Öbek during embryogenesis. In stage 16 wild-type embryos, Öbek is weakly expressed in the cytoplasm of glial, neuronal and epidermal cells (Fig. 3A, e.g. ePG2, arrowhead and asterisk, respectively). In contrast, a strong nuclear expression is observed in a subset of glial nuclei in the PNS, as well as in the CNS and in the nuclei of the oenocytes (OE) (Fig. 3A). In the peripheral nerves, Öbek is most strongly expressed by embryonic peripheral glial cells (ePG3, ePG4, ePG7), which give rise to the SPGs, and is weakly expressed in ePG12, which gives rise to the glia of the transverse nerve (von Hilchen et al., 2008). Similarly, *Mz97-Gal4*, inserted in the *öbek* locus, also labels the ePG3, ePG4, ePG7, ePG12 and the OE (Fig. 3B). Thus, the expression pattern seen in *Mz97-Gal4 UAS-Lam::GFP* animals recapitulates the domains of strong *öbek* expression.

During larval stages, strong nuclear Öbek expression persists in the SPGs (Fig. 3C). All Öbek expression in nerves is removed following panglial knockdown of *öbek* (Fig. S4A,B). *Gli-Gal4*-mediated *öbek* knockdown, however, removes only the strong nuclear Öbek in SPGs, and a uniform cytoplasmic Öbek expression remains along the nerve (Fig. S4A,C). Thus, differential expression of Öbek can be noted in the different glial subtypes.

Öbek expression in glial cells is crucial for survival

We next generated a small deficiency ($öbek^{\Delta}$) removing *öbek* and the adjacent gene *CheA56a* using FRT/Flp-mediated recombination (Parks et al., 2004) (Fig. 4A). *CheA56a* is expressed only in adult stages (FlyBase) and a transposon insertion into the open reading frame of this gene is homozygous viable and larval glial cells are normal ($CheA56a^{LL01319}$). Animals homozygous for the $öbek^{\Delta}$ allele are late embryonic lethal. They show no detectable Öbek protein and have no obvious developmental abnormalities during embryonic stages (Fig. S5). However, animals carrying the $öbek^{\Delta}$ allele in trans to the *Mz97-Gal4* insertion are viable but show a nerve-bulging phenotype, which is comparable to the phenotype of homozygous *Mz97-Gal4* animals (data not shown). A MiMIC insertion (Nagarkar-Jaiswal et al., 2015; Venken et al., 2011) in the *öbek* gene also leads to late embryonic lethality when homozygous or in trans to $öbek^{\Delta}$ (Fig. 4A, $Mi\{MIC\}^{02644}$).

öbek encodes two distinct protein isoforms, which differ only in their last three amino acids [Fig. 4A, nomenclature of the different

Development (2018) 145, dev164111. doi:10.1242/dev.164111

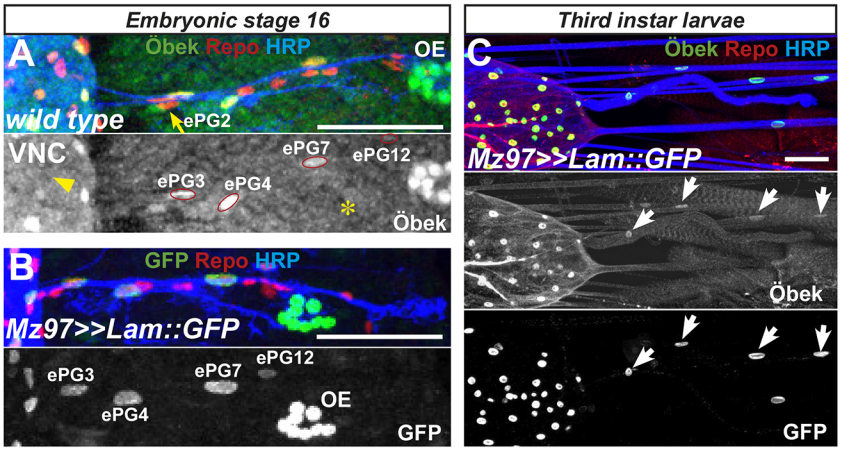

Fig. 3. Expression of Öbek. (A) In wild-type stage 16 embryos, strong nuclear Öbek expression can be detected in several peripheral glial cells (ePG3, ePG4, ePG7 and ePG12; *n*>10 embryos) and in the oenocytes (OE). A general cytoplasmic expression is detected in other peripheral glial cells including ePG2 (yellow arrow), the ventral nerve cord (arrowhead) and the epidermis (asterisk). (B) Stage 16 embryo expressing GFP under the control of *Mz97-Gal4* (*Mz97-Gal4, UAS-Lamin::GFP*). The nuclei of ePG3,4,7 and 12 as well as the oenocytes (OE) are labeled. (C) Third-instar larvae, showing nuclear GFP reporter expression under the control of *Mz97-Gal4* (*Mz97-Gal4, UAS-Lamin::GFP*). Nuclear Öbek expression colocalizes with the Mz97-Gal4-positive nuclei (white arrows). Scale bars: 50 µm.

isoforms (PA/B and PC/D) according to FlyBase]. To further test whether the early lethality of the deletion or the MiMIC insertion allele represents the amorphic phenotype of *öbek*, we performed rescue experiments with the Öbek$^{PA/B}$ isoform. Ubiquitous re-expression of this protein shifts the lethal phenotype associated with the homozygous deficiency from embryonic stages to late pupal stages (*öbek*$^{\Delta/\Delta}$*; tub-Gal4, UAS-öbek*, Table 1). Next, we performed glia-specific rescue experiments using *repo-Gal4*. As noted for ubiquitous expression, re-expression of *öbek* only in glial cells rescued the embryonic lethal phenotype of *öbek*$^{\Delta}$ mutants and pharate adults developed. This clearly demonstrates a vital glial requirement for *öbek*. In line with this notion, we failed to observe

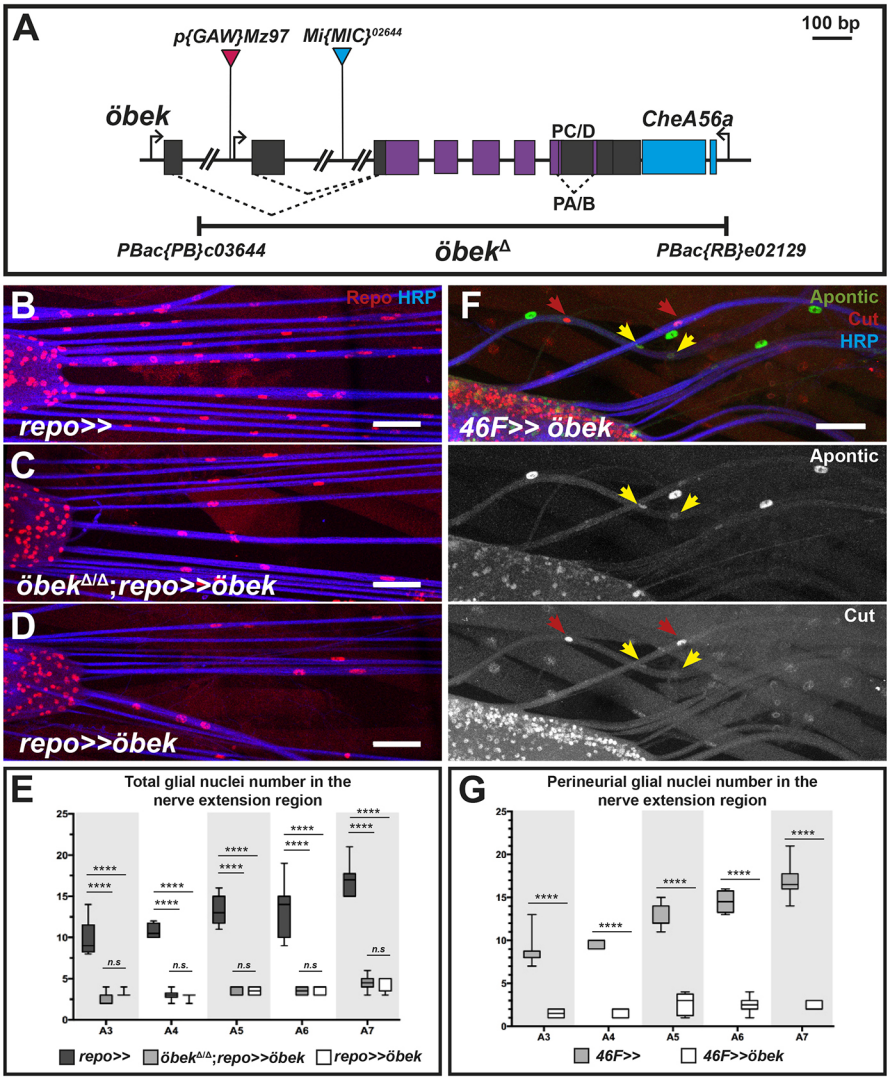

Fig. 4. High Öbek expression in perineurial glia blocks proliferation. (A) *öbek* gene locus. The *P{GAW}Mz97* insertion is located ∼100 bp upstream of the second transcriptional start site within the first intron, which is ∼15 kb in size. A second transcriptional start site is located within this intron ∼5 kb further downstream of the first promoter. The *Mi{MIC}*^{02644} insertion, which most likely represents a null mutant of *öbek*, is located ∼5 kb upstream of the third exon. The extent of the *öbek* deficiency allele (*öbek*$^{\Delta}$) is indicated. It covers most of the *öbek* locus and the gene *CheA56a*. (B-D) Confocal projections of third-instar larval filet preparations stained as indicated. The ventral nerve cord is to the left. The first 400 µm of the abdominal nerves are shown. (B) Control larva. (C) *öbek*-deficient larva rescued by panglial re-expression of *öbek* show reduced numbers of peripheral glial nuclei. (D) Panglial overexpression of *öbek* in otherwise wild-type animals also causes a reduced number of glial nuclei. The quantification is shown in E. (E) Total number of glial nuclei along the NER of the segmental nerves A3-A7 was quantified for the indicated genotypes ($n \geq 7$ nerves for each abdominal nerve). (F) Apontic is expressed in perineurial and subperineurial nuclei, whereas Cut is expressed in subperineurial and wrapping nuclei. Upon overexpression of *öbek* in the perineurial glial cells using 46F-Gal4 only few perineurial glial cells remain, whereas subperineurial and wrapping glial cells persist (yellow and red arrows, respectively). (G) Quantification of perineurial glial-specific knockdown. The number of perineurial glial nuclei is reduced to one to two cells per NER. Scale bars: 50 µm. n.s., not significant; ****$P \leq 0.0001$.

Development (2018) 145, dev164111. doi:10.1242/dev.164111

Table 1. Rescue experiments

Background	Driver	Driver type	Lethality shift	GNN in the NER
öbek$^{\Delta}$ + *UAS-öbek*	*tubulin-Gal4*	Ubiquitous	From embryo to late pupa	Reduced
	repo-Gal4	Panglial	From embryo to late pupa	Reduced
	tubulin-Gal4, repo-Gal80	Ubiquitous except glia	No lethality shift	NA
	SPG-Gal4	Subperineurial glial	No lethality shift	NA
	Gli-Gal4	Subperineurial glial	No lethality shift	NA
	repo-Gal4, moody-Gal80	Panglial except subperineurial glia	No lethality shift	NA

The *UAS-öbek* transgene was expressed in an *öbek*-deficient background using different Gal4 and Gal80 lines as indicated. *n*=5 independent crosses for each genotype. NA, not analyzed; GNN, glial nuclei number.

any rescue when *öbek* was re-expressed in all cells except in glial cells (*öbek*$^{\Delta/\Delta}$*; tub-Gal4, repo-Gal80, UAS-öbek*, Table 1). Such animals were still embryonic lethal.

We then generated a *moody-Gal80* strain to exclude Gal4-mediated gene activation specifically in the SPGs, while activating expression in all other glial cells using *repo-Gal4*. In such animals (*öbek*$^{\Delta/\Delta}$*; repo-Gal4, moody-Gal80, UAS-öbek*), no rescue of the embryonic lethality associated with *öbek*$^{\Delta/\Delta}$ was observed and animals did not leave the egg cases. We thus conclude that *öbek* expression is essential in the SPGs for survival (Table 1). We also performed rescue experiments using the *Gli-Gal4* or *SPG-Gal4* driver lines, but in both cases no shift in the lethal phase was noted, suggesting that Öbek function is crucial in perineurial glial cells (Table 1).

High Öbek levels block proliferation in perineurial glia

Because suppression of *öbek* results in an increase in glial nuclei number, we wondered whether rescued animals show normal numbers of glial nuclei. Panglial rescue of *öbek*$^{\Delta}$ using either isoform (*öbek*$^{\Delta}$*/öbek*$^{\Delta}$*; repo-Gal4, UAS-öbek*) results in a severe reduction in the number of Repo-positive glial nuclei (Fig. 4B,C,E). Interestingly, a similar phenotype was noted in animals in which *öbek* overexpression was induced in glial cells through a *UAS-öbek* transgene (Fig. 4D,E). Öbek overexpression does not affect Cut-expressing nuclei (wrapping glia and SPGs) but reduces the number of Apontic-positive nuclei (perineurial glia), indicating that perineurial glial nuclei number was significantly reduced (data not shown). Similarly, we noted a reduced number of Apontic-positive nuclei but normal numbers of Cut-expressing nuclei when we overexpressed Öbek specifically in the perineurial glia using *46F-Gal4* (Fig. 4F,G). Therefore, we conclude that Öbek overexpression affects only the number of perineurial glial cells, which are the sole mitotically active glial cells along peripheral nerves. Similarly, Öbek overexpression affects also the cell division of the perineurial glial cells associated with the eye imaginal disc and the CNS (Fig. S6A,B).

To test whether Öbek affects all dividing cells, we expressed Öbek in neuroblasts using the *insc-Gal4* driver or during wing imaginal disc development employing the *en-Gal4* driver, which activates gene expression only in the posterior compartment of the imaginal disc. Expression of Öbek can be detected using specific antibodies. Surprisingly, expression of *öbek* in neuroblasts using the *insc-Gal4* driver did not interfere with the normal division pattern of neuroblasts and brains appeared to have a normal size (Fig. S6C,D). Likewise, no change in cell number is noted upon *öbek* expression in the imaginal disc epithelium as detected by DAPI labeling (Fig. S6E). This indicates that high Öbek expression blocks proliferation only in glial cells.

N-terminal asparagine amidohydrolase function of Öbek in glia

Öbek is highly conserved among the Drosophilidae and related to the mammalian N-terminal asparagine amidohydrolase 1 (NTAN1, 38% identity at amino acid level). The mammalian NTAN1 enzyme is involved in the N-end rule pathway, controlling degradation of proteins with destabilizing N-terminal amino acids such as Asn or Gln. NTAN1 catalyzes the generation of an N-terminal aspartate that is the substrate of the arginine transferase Ate1, which thereby triggers ubiquitination and subsequent proteasomal degradation (Fig. 5A) (Bachmair et al., 1986; Sriram et al., 2011).

To test whether Öbek indeed acts in the N-end rule pathway in glial cells (Ditzel et al., 2003), we generated two constructs that encode reporter proteins, which upon proteolytic cleavage expose either a stabilizing amino acid (methionine, Ub-Met-GFP) or a destabilizing amino acid (asparagine, Ub-Asn-GFP) at the N-terminus of a GFP moiety, following a described strategy (Dantuma et al., 2000) (Fig. 5B). We generated transgenic flies carrying the respective constructs in the same landing site to ensure comparable expression levels.

When we expressed the Ub-Met-GFP reporter protein in all glial cells using *repo-Gal4*, we noted strong signals in peripheral nerves (Fig. 5C). Likewise, stable expression of Ub-Met-GFP was noted when we expressed the reporter only in the perineurial glial cells, or the wrapping glia or the SPGs, using *46F-Gal4*, *nrv2-Gal4* or *Gli-Gal4*, respectively (Fig. 5D-F). In contrast, we noted no GFP signals when we expressed the predicted N-terminal asparagine amidohydrolase substrate, Ub-Asn-GFP, in all glial cells or subsets of glial cells (Fig. 5G-J). This suggests that the N-end rule pathway operates in all *Drosophila* glial cells and its activity can be determined by comparing the expression of Ub-Met-GFP and Ub-Asn-GFP.

To assay the influence of Öbek on the stability of N-end rule pathway reporters, we silenced *öbek* expression. Intriguingly, panglial suppression of *öbek* leads to detectable expression of Ub-Asn-GFP, indicating that Öbek functions in the N-end rule pathway and is required to destabilize the Asn-GFP reporter (Fig. 5K). Because subtype-specific knockdown also led to stabilization of GFP signals in perineurial and wrapping glial cells (Fig. 5L,M), we conclude that Öbek protein is found and acts also in wrapping and perineurial glial cells. Only SPGs, which express the highest levels of Öbek were refractive to the *öbek* downregulation and Ub-Asn-GFP is still undetectable (Fig. 5N). However, expression of a dominant-negative form of valosin-containing protein (VCP; TER94) (Rumpf et al., 2011), which interferes with proteasomal degradation (Meyer et al., 2012; Rumpf et al., 2011, 2014; Wójcik et al., 2006), could stabilize Asn-GFP in SPGs (Fig. S7A,B). Moreover, VCP^{QQ} occasionally caused nerve bulges (Fig. S7C). Taken together, these data suggest that the N-end rule pathway member Öbek operates in peripheral *Drosophila* glia, where it controls ploidy in the large SPGs.

Development (2018) 145, dev164111. doi:10.1242/dev.164111

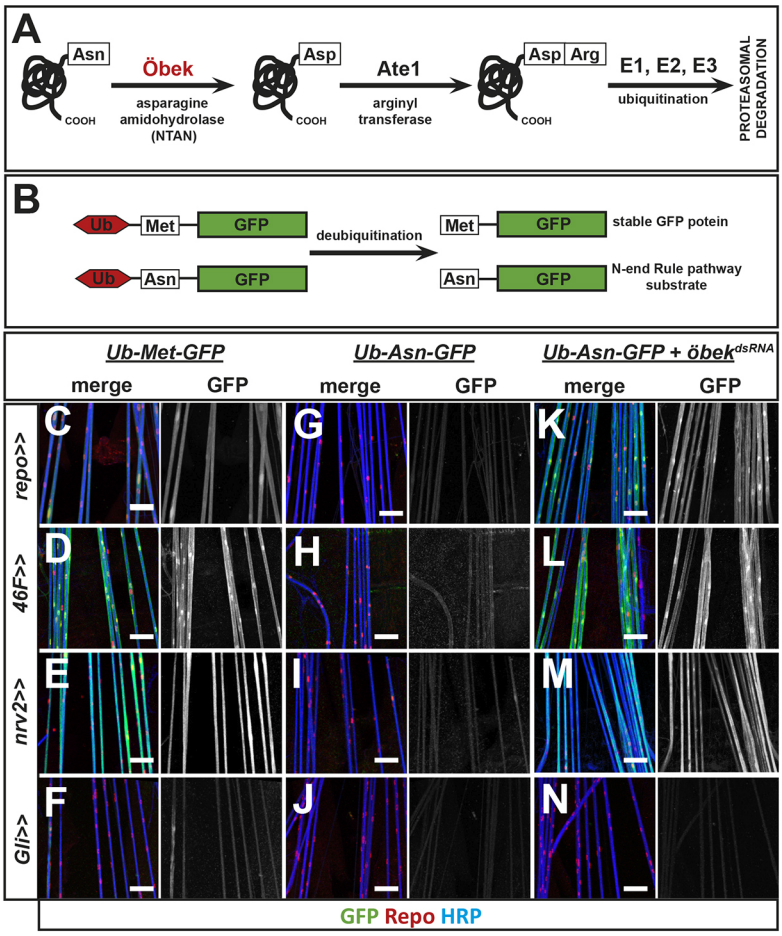

Fig. 5. Öbek acts as an asparagine amidohydrolase in the N-end rule pathway. (A) Proposed activity of Öbek in the N-end rule pathway. Öbek encodes a predicted N-terminal asparagine amidohydrolase acting in the N-end rule pathway. This enzyme recognizes proteins with an N-terminal destabilizing asparagine (Asn) residue and hydrolyzes it into aspartate (Asp). The N-terminal Asp is further processed by the Arginyl-transferase enzyme, Ate1, which conjugates an Arginine (Arg) to the N-terminus to generate a potential substrate for subsequent ubiquitination and proteasomal degradation. (B) GFP reporters to detect N-end rule pathway activity. Ubiquitin-GFP chimera carrying a deubiquitination signal sequence are deubiquitinated enabling the exposure of the N-terminal amino acids at the N-terminus of the GFP protein. Methionine (Met) at the N-terminus leads to a stable GFP-reporter, whereas an Asn renders the GFP reporter instable. (C-N) Confocal projections of third instar larval peripheral nerves stained as indicated. The images are taken ~100 µm posterior to the ventral nerve cord. (C-F) Expression of the Ub-Met-GFP reporter in all glia (*repo>>*) (C), perineurial glia (*46F>>*) (D), wrapping glia (*nrv2>>*) (E), or in SPG (*Gli>>*) (F). In all cases, GFP expression can be detected in the peripheral nerves. (G-J) Expression of the Ub-Asn-GFP reporter in the same sets of glial cells as in C-F. No GFP can be detected, indicating the instability of the Ub-Asn-GFP reporter. (K-N) Upon concomitant suppression of *öbek* expression, Ub-Asn-GFP is stabilized and can be detected in all glial subtypes except for the SPGs. Scale bars: 50 µm.

To further test the role of the N-end rule pathway in glial cells we analyzed the enzymatic function downstream of Öbek. *Ate1* encodes an arginine transferase and routes Öbek targets towards proteasomal degradation (Sriram et al., 2011) (Fig. 5A). The $Ate1^{k10809}$ insertion mutant, which affects all Ate1 isoforms, results in early larval lethality precluding an analysis of third-instar larval nerves. *Ate1* knockdown stabilizes the Asn-GFP reporter in glial cells, but does not lead to nerve bulges or increased number of glial nuclei (Fig. S7F-H), which is likely due to inefficient *Ate1* knockdown through RNAi. In the same line, whereas *Ate1* mutants are lethal ubiquitous, knockdown of *Ate1* using four different double-stranded RNA (dsRNA) lines does not cause lethality. Intriguingly, a nerve-bulging phenotype was noted upon silencing of two proteasomal subunits, *prosα7* and *prosß5*, in SPGs (Fig. S7D,E).

Öbek counteracts FGF and Hippo signaling

Prominent regulators of cell size control are members of the receptor tyrosine kinase (RTK) family, such as the Insulin receptor, the EGF receptor or the FGF receptor, and the Hippo pathway. Both RTK and Hippo signaling systems can be linked through the MAPK pathway (Reddy and Irvine, 2013). Moreover, constitutively active Heartless (an FGF receptor in *Drosophila*), as well as overactivation of the Hippo pathway through constitutively active Yorkie (Yki^{S168A}), is known to promote glial cell proliferation (Avet-Rochex et al., 2012; Franzdóttir et al., 2009; Reddy and Irvine, 2011).

We wanted to determine whether peripheral glia can respond to Yorkie and Heartless signaling. We expressed constitutively active Yorkie (Yki^{S168A}) and constitutively active FGF receptor Heartless (*λhtl*) in SPGs and perineurial glial cells (Fig. S8A-C). In both cases, an increase in the number of glial nuclei of the respective subtype can be detected. Moreover, concomitant suppression of *öbek* in the perineurial glia greatly enhances this phenotype (Fig. S8B,C). Upon co-expression of $öbek^{dsRNA}$ and activated *htl* or *yorkie* in SPGs, wild-type numbers of nuclei were noted, possibly due to the fact that the *Gli-Gal4* driver is not strong enough to evoke sufficient expression levels of both transgenes. We therefore switched to *repo-Gal4*, which is strongly active in both glial cell types.

Panglial expression of the constitutively active Yorkie (Yki^{S168A}) protein results in prominent nerve bulges accompanied by an increased number of glial nuclei, with the longest nerves being the most strongly affected (Fig. 6A, compare with Fig. 1; for quantification see Fig. 6I). Intriguingly, overexpression of Öbek reverts this phenotype (Fig. 6A,B,I), whereas suppression of *öbek* aggravates it (Fig. S8D). When we silenced *yorkie* expression using RNAi, we noted fewer glial nuclei (Fig. 6C,I). Concomitant silencing of *öbek* does not significantly change the reduced glial nuclei number and no nerve bulges are observed (Fig. 6D,I). Thus, *öbek* genetically interacts with *yorkie* in glial cells.

Next, we expressed activated Heartless (*λhtl*, FGF receptor) in a panglial manner. This also causes an increase in the number of glial nuclei in bulged areas (Fig. 6E,J). Interestingly, however, the shortest nerves A3 and A4 appear to be more affected compared with longer nerves (Fig. 6J). As noted before for the Yorkie-induced glial phenotype, we found that concomitant overexpression of Öbek

Development (2018) 145, dev164111. doi:10.1242/dev.164111

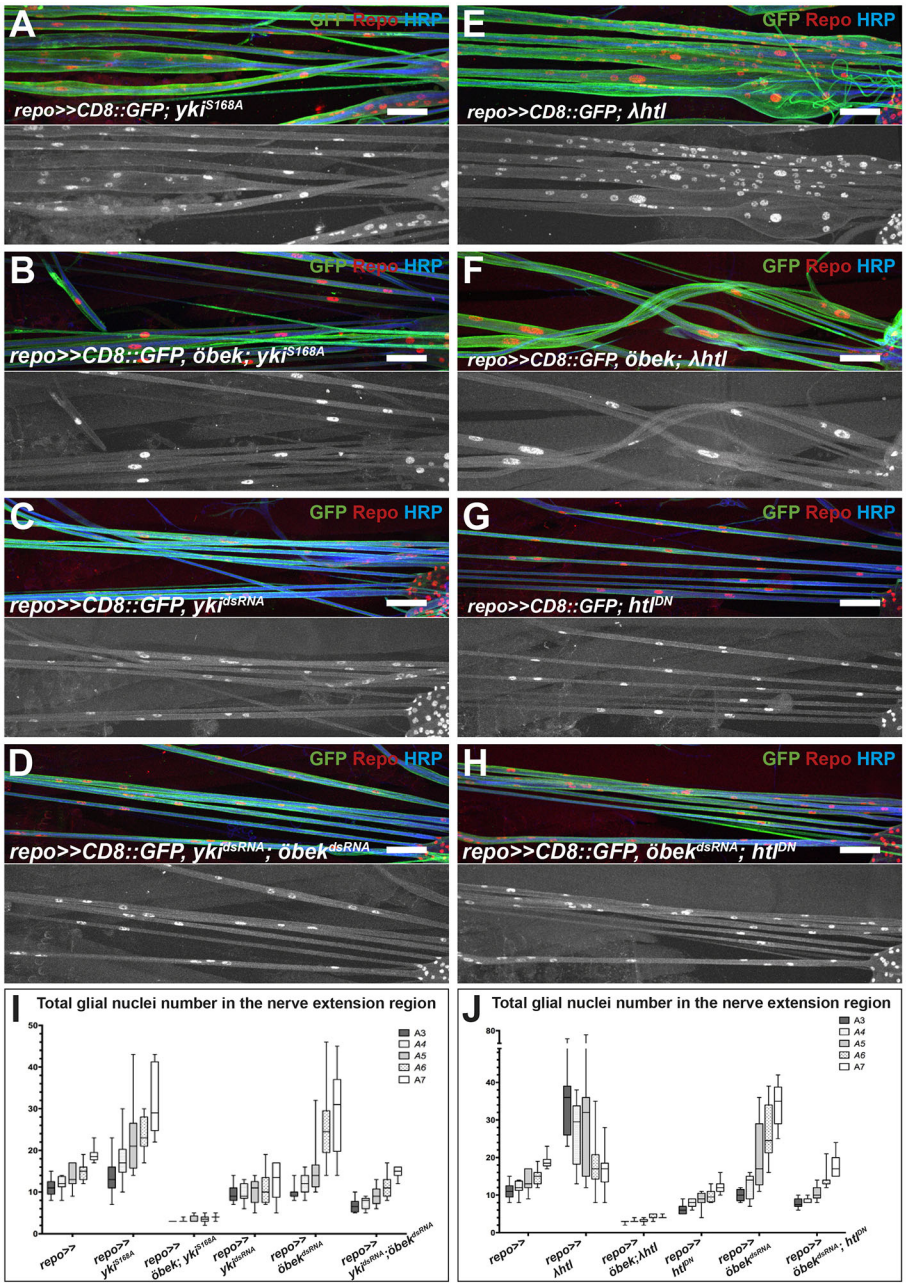

Fig. 6. Öbek counteracts FGF and Hippo signaling. Confocal projections of third instar larval filet preparations stained as indicated. Nerve regions directly posterior to the ventral nerve cord are shown. The ventral nerve cord is to the right. For wild type see Fig. 1. (A) Panglial expression of a constitutively-active form of Yorkie (*yki*^{S168A}) leads to nerve swellings and an increased number of glial nuclei. For quantification see I (A3, *P*=0.05; A4, *P*=0.005; A5, *P*=0.004; A6, *P*=0.000001; A7, *P*=0.0001). (B) Concomitant expression of Yki^{S168A} and Öbek shows the Öbek gain-of-function phenotype with reduced numbers of glial nuclei compared with wild type (see I for quantification; all nerves *P*<10^{-8}). (C) Suppression of *yorkie* expression leads to a reduced number of glial cell nuclei (A3, *P*=0.2; A4, *P*=0.05; A5, *P*=0.02; A6, *P*=0.01; A7, *P*=0.001). (D) Although suppression of *öbek* results in an increase in glial nuclei number (third chromosomal insertion, see Fig. S1A), concomitant suppression of *yorkie* and *öbek* expression results in a reduced number of glial nuclei when compared with wild type, mimicking the *yorkie* suppression situation (see I for quantification; all nerves *P*<0.005). (E) Panglial expression of constitutively active FGF receptor Heartless (*λhtl*) leads to nerve swellings and an increased number of glial nuclei (arrows) (see J for quantification; A3, *P*=10-6; A4, *P*=0.0002; A5, *P*=0.01, A6 and A7, n.s.). (F) Concomitant expression of activated Heartless and Öbek shows the Öbek gain-of-function phenotype with dramatically reduced glial nuclei numbers (see J for quantification; all nerves *P*<0.0002). (G) Expression of a dominant-negative form of the FGF receptor Heartless (*htl*^{DN}) leads to reduced numbers of glial nuclei (see J for quantification; all nerves: *P*<0.0001). (H) Co-expression of *htl*^{DN} and *öbek*^{dsRNA} (second chromosomal insertion) results in a reduced number of glial nuclei compared with wild type, mimicking panglial expression *of htl*^{DN} (see J for quantification; A3, *P*=0.0008; A4, *P*=0.0007; A5, *P*=0.02; A6 and A7, n.s.). (I,J) Quantifications of the glial nuclei numbers in the NER for the genotypes in A-H. Scale bars: 50 µm.

completely blocks the effect of activated Heartless on glial nuclei number and reverts it (Fig. 6F,J), whereas concomitant suppression of *öbek* aggravates this phenotype (Fig. S8E). When we suppressed *heartless* function in all glial cells by expressing a dominant-negative FGF receptor (*htl*^{DN}), we noted a reduced number of glial cell nuclei number along all abdominal nerves; therefore, reduced Heartless function interferes with glial proliferation (Fig. 6G,J). Concomitant knockdown of *öbek* does not change this phenotype and no nerve bulges are observed (Fig. 6H,J; note that different *öbek*^{dsRNA} constructs were used in the experiments). Thus, we conclude that Öbek genetically interacts with the FGF signaling pathway to counteract its activity.

In summary, we conclude that high Öbek levels in SPGs suppress the activities of FGF and Hippo signaling (propogated through Heartless and Yorkie, respectively), thereby limiting endoreplication and consequent cell growth (Fig. 7). Owing to the high levels of Öbek, SPGs are less responsive to modulation of Heartless and Yorkie activities. Perineurial glial cells, on the other hand, express moderate levels of Öbek and thus are more responsive to elevated levels of Heartless and Yorkie activities, hence adjusting perineurial cell number during growth of the animal (Fig. 7). In conclusion, *öbek* counteracts signals propagated through *yorkie* and *heartless* activities in regulating cell growth and DNA replication in glial cells of the blood-brain barrier (Fig. 7).

DISCUSSION

How do cells accomplish changes in body size during development? Some cells keep their size constant and initiate proliferation, whereas other cells start to grow and may become polyploid. Such antithetic growth strategies are realized by the two glial cell types of the *Drosophila* blood-brain barrier. The perineurial glial cells initiate a proliferative response to match the growth of the nervous

Development (2018) 145, dev164111. doi:10.1242/dev.164111

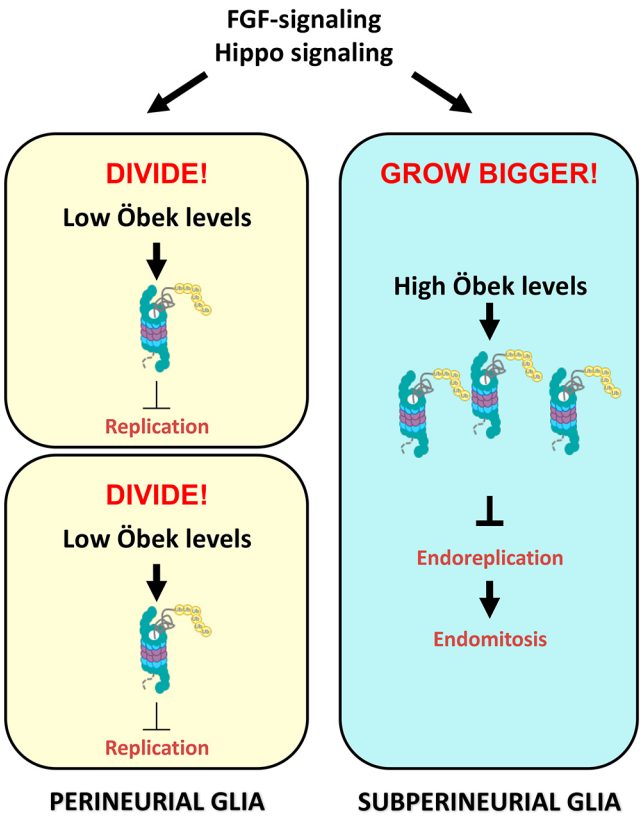

Fig. 7. Model of Öbek function in peripheral glial cells. Schematic view of perineurial glial cells and SPGs, which differently interpret common growth signals (FGF and Hippo signaling). The perineurial glia divide during development and have low cytoplasmic Öbek expression, which weakly suppresses replication rates and proliferation. The SPGs, in contrast, do not divide but the cells grow in size and undergo endoreplication. High levels of nuclear Öbek are needed to constrain endoreplication rates and limit endomitosis.

system during larval development, whereas the SPGs do not divide, but rather expand in size and become polyploid. Here, we have shown that differential expression of the N-end rule pathway component Öbek accounts for this differential response to common signals governing cell size regulation (Fig. 7).

We identified the N-end rule pathway component Öbek as a crucial glial factor for adjusting the replication rates to extrinsic and intrinsic growth signals. The N-end rule pathway is found in all eukaryotes. Therefore, we expected that members of this protein destabilization pathway would be equally expressed in all cell types, including glia, as found in mice (Grigoryev et al., 1996; Kwon et al., 1998; Zhang et al., 2014). Surprisingly, however, we found a differential localization of Öbek during *Drosophila* development. Next to a weak uniform cytoplasmic expression in many tissues, we noted a strong nuclear expression in SPGs, which are polyploid cells and can undergo endomitosis (Unhavaithaya and Orr-Weaver, 2012). Why Öbek localizes to the nuclei in the SPG is unclear. To some extent, it might correlate with the ploidy status of the cell because nuclear Öbek is also found in other polyploid cell types, such as salivary gland cells and the OE (Cinnamon et al., 2016; Edgar et al., 2014; Orr-Weaver, 2015). However, polyploid wrapping glial nuclei do not show strong nuclear Öbek expression, suggesting additional cell type-specific regulatory mechanisms.

Interestingly, not all mitotically active tissues appear to be sensitive to high Öbek expression. In the wing disc epithelium – where the N-end rule pathway is active to destabilize the Asn-GFP reporter – overexpression of Öbek does not cause any abnormal phenotypes. Likewise, expression of Öbek in neuroblasts does not cause any change from the normal division pattern. In fact, *öbek* mutants, which die as late embryos, can be rescued to late pupal stages by re-expression of *öbek* only in glial cells. Such rescued animals show no nerve bulges, but rather a reduced number of perineurial glial cells, owing to the resulting Öbek gain of function in perineurial glial cells. This probably also accounts for the late pupal lethality, because these cells are needed to metabolically support neurons of the *Drosophila* nervous system (Volkenhoff et al., 2015).

To further understand *öbek* function, we tested the relevance of signaling pathways – Hippo and FGF – controlling glial cell size and proliferation in the *Drosophila* nervous system (Avet-Rochex et al., 2012; Franzdóttir et al., 2009; Reddy and Irvine, 2011, 2013). In the central nervous system, Yorkie, an essential transcriptional activator implementing Hippo pathway activity, is required to establish the correct ploidy. Moreover, it is post-transcriptionally regulated, in part, through *miR-285* which, when depleted, results in increased SPG ploidy (Li et al., 2017). Here, we have shown that Yorkie also regulates the number of glial nuclei in peripheral glia. Intriguingly, Öbek counteracts Yorkie and can suppress glial phenotypes induced by constitutively active Yorkie (Yki^{S168A}). More importantly, the *öbek* loss-of-function phenotype, which is primarily caused by additional SPG nuclei, can be suppressed by co-suppression of *yorkie* activity, suggesting a genetic interaction between the two in regulating glial growth both in the perineurial glial cells and the SPGs.

The *Drosophila* FGF receptor, Heartless, is needed during peripheral glial proliferation and migration (Franzdóttir et al., 2009; Sieglitz et al., 2013). Similar to Yorkie, Öbek genetically interacts with Heartless and restricts its activity (Fig. 7). This might be caused by N-end rule pathway targeting important regulator(s) in these signaling cascades. In fact, the MAPK Rolled has recently been reported to be a putative N-end rule pathway substrate (Ashton-Beaucage et al., 2016).

The increased rate of DNA synthesis is thought to match the growing metabolic demands as the SPGs become very large during development (Awasaki et al., 2008; Schwabe et al., 2005; Silies et al., 2007; Stork et al., 2008; Unhavaithaya and Orr-Weaver, 2012). In fact, cell division of these cells is suppressed because the blood-brain barrier needs to stay intact during the entire lifecycle (Bainton et al., 2005; Mayer et al., 2009; Volkenhoff et al., 2015). However, surprisingly, when we compared the C-value of the SPGs found along different segmental nerves, we were unable to find a clear correlation between cell size and DNA content, suggesting that this regulation is not very strict and different than in, for example, salivary glands, where all cells reach a comparable ploidy (Edgar et al., 2014).

The variable C-value of wild-type SPGs might explain why this cell type is very sensitive to the loss of *öbek*. If an SPG is affected, nerve bulging correlates with an increased rate of endoreplication, which results in the appearance of multiple nuclei. *öbek* knockdown only in perineurial glia causes only mild proliferation defects in long nerves. However, when we challenge these cells by activating Yorkie or Heartless, *öbek* function becomes visible in perineurial glial cells of all nerves. Therefore, we propose that the normal function of Öbek is to restrict replication in response to growth signals in the cells of the blood-brain barrier (Fig. 7). Large polyploid cells, such as the SPGs, might rely more heavily on these signals, and thus they express high levels of Öbek during development. In contrast, proliferative perineurial glial cells express only moderate levels, and they do not tolerate high levels of Öbek because there is a dramatic reduction in their nuclei number observed upon Öbek overexpression.

Development (2018) 145, dev164111. doi:10.1242/dev.164111

In conclusion, in the peripheral nervous system, the predicted N-end rule pathway component Öbek is differentially expressed by glial cells of the blood-brain barrier. We propose a model in which high Öbek levels are crucial in SPGs to limit propagation of growth signals mediated, at least in part, by Heartless and Yorkie to limit endoreplication and the consequent appearance of extra nuclei. Perineurial glial cells express moderate levels of Öbek, ensuring that growth signals efficiently mediate proliferation during larval development (Fig. 7).

MATERIALS AND METHODS

Generation of *Drosophila* lines

For Gal4-directed expression of transgenes, *pUASt-attB-rfa* vector was used (Rodrigues et al., 2012). Complementary DNA was amplified from wild-type larval mRNA, verified by sequencing and used as a template to amplify the *öbek* coding sequence (CDS). *Ub-Met-GFP* and *Ub-Asn-GFP* were generated through PCR by introducing a methionine (M) or asparagine (N) and a linker sequence GKLGRQ between the ubiquitin- and eGFP-coding sequences. All constructs were generated by Golden Gate cloning, and were inserted into the *86Fb* landing site. The *UAS-öbek* construct was also inserted in the landing site *44F* (Bischof et al., 2007). *moody-Gal80* was generated by amplifying the 2.4 kb fragment of genomic DNA directly upstream of the *moody* open reading frame using the sense primer 5′-CACCCTACGTCTTCAGTTCGATA-3′ and the antisense primer 5′-GCTCAGGCTCTGGTAAGAAATAAA-3′ (Schwabe et al., 2005), cloned into a pBPGUwattBGal80 plasmid that was generated from pBPGUwGal4 (Addgene) and inserted in the *86Fb* landing site. The $öbek^{\Delta}$ deficiency allele was generated by FRT-Flp-mediated recombination using the PBac elements *PBac{PB}c03644* and *PBac{RB}e02129* (Parks et al., 2004).

Drosophila genetics

All fly work was conducted according to standard procedures and all crosses were performed at 25°C. We screened ∼5000 dsRNA-expressing lines for lethality when expressed in a panglial manner (Schmidt et al., 2012). Approximately 750 lines caused lethality. Of these lines, we screened ∼400 for phenotypes in the abdominal nerves (R.K., unpublished). The following lines were obtained from public *Drosophila* stock centers [Vienna Drosophila Resource Center (VDRC) and Bloomington *Drosophila* Stock Center (BDSC)]: $CG5473(öbek)^{dsRNA(II)}$ (VDRC 105482), $CG5473(öbek)^{dsRNA(III)}$ (VDRC 21567), $Ate1^{dsRNA}$ (VDRC 28111, 28112 and 104360, BDSC 53867), $Ate1^{k10809}$ (BDSC 11001). *UAS-stingerRed* (BDSC 8546), $mcherry^{TRIP}$ (BDSC 35785), *UAS-mCD8::GFP* (BDSC 5137), *FUCCI* (BDSC 55122), yki^{TRIP} (BDSC 34067), $UAS\text{-}yki^{S168A.V5}$ (BDSC 28818) *UAS-lamGFP* (BDSC 7378), *repo-Gal4*, *Gli-Gal4* (Sepp and Auld, 1999), *SPG-Gal4* (Stork et al., 2008), *Mz97-Gal4* (Ito et al., 1995), *insc-Gal4* (kindly provided by C. Berger, Institute of Genetics, Mainz, Germany), *tub-Gal4* (BDSC 5138), *nrv2-Gal4* (BDSC 6797), *engrailed-Gal4* (BDSC 30564), *repo-Gal80* (Awasaki et al., 2008), $UAS\text{-}htl^{DN}$ and *UAS-λhtl* (Franzdóttir et al., 2009; Michelson et al., 1998). For multicolor stochastic labeling, *MCFO-2* flies (Nern et al., 2015) were crossed to glial subtype-specific Gal4 drivers. *hsFlp*-induced recombination within the MCFO-2 was induced by a 1 h heatshock at 37°C in 96-h-old larvae.

Immunostaining and imaging

Overnight embryo collections were fixed as described (Edenfeld et al., 2006; Xu et al., 1999). Fixation and preparation of eye and wing imaginal discs for immunohistochemistry were performed as described (Yuva-Aydemir et al., 2011). Larval filets were prepared as described and fixed for 3 min in Bouin's solution and immunostained (Matzat et al., 2015). Antibodies used were as follows: mouse anti-Repo [1:5; Developmental Studies Hybridoma Bank (DSHB)], mouse anti-Cut (1:10; DSHB), mouse and rabbit anti-GFP (1:1000; Molecular Probes), rabbit anti-Apontic (1:200; Eulenberg and Schuh, 1997) and anti-HRP 649 (1:500; Jackson ImmunoResearch Laboratories) and rabbit anti-DsRed (1:1000, Abcam). Rabbit anti-Öbek antiserum was used at 1:100. All conjugated secondary antibodies (Invitrogen) were used at 1:1000. Specimens were analyzed using a Zeiss 710 LSM or Zeiss 880 LSM; images were processed using the Zeiss LSM imaging software or Fiji software.

Statistical analyses

Nuclear number and DNA content were quantified on fixed and stained larval filet preparations. Nuclear counts were performed manually by inspecting the entire nerve length in tiled images of the entire animal generated at a confocal microscope. DAPI staining was performed at 100 ng/ml DAPI in 1× PBS containing 0.1% Triton X-100 for 2 h at room temperature. The amount of DNA was quantified in the relevant *Z*-stacks by determining the DAPI fluorescence intensity using the 'measurements' function in Fiji software. The corrected total integrated density (CTCF) was calculated for each nucleus using the following function: CTCF=integrated density – (area of selected nucleus × mean fluorescence of background readings). Background readings were made by measuring the fluorescence three times in regions in which no nuclei were present. Ploidy was then calculated by normalizing each SPG nucleus to an Elav-positive diploid neuron in the ventral nerve cord, imaged on the same nervous system with the same laser settings. Given values are the total C-values of all SPG nuclei on a given NER. To determine the statistical significance of the nuclear number, we performed a two-tailed, unpaired Student's *t*-test, and to analyze the C-values we employed a Mann–Whitney test because the data were found to be non-normally distributed (D'Agostino–Pearson omnibus test in GraphPad Prism was used). All box plots were generated using GraphPad Prism.

Acknowledgements

We are thankful to the *Drosophila* stock centers for providing many fly stocks needed to conduct this study; C. Berger for providing *insc-Gal4*; and I. Hariharan, K. Irvine and R. Schuh for providing antibodies. F. Langen performed some of the initial RNAi experiments; V. Simon participated in the generation of the N-end rule reporters. We thank S. Luschnig, S. Schirmeier, R. Stanewsky and G. Steffes for critical discussion of the manuscript.

Competing interests

The authors declare no competing or financial interests.

Author contributions

Conceptualization: S.Z., C.K.; Methodology: S.Z., F.S., S.R.; Formal analysis: S.Z., C.K.; Investigation: S.Z., F.S., R.K.; Resources: F.S., R.K., B.A., S.R.; Writing - original draft: S.Z.; Writing - review & editing: S.Z., C.K.; Visualization: S.Z.; Funding acquisition: C.K.

Funding

This work was supported by Deutsche Forschungsgemeinschaft [SFB629 to C.K.] and by the Graduate School of the Cells-in-Motion Cluster of Excellence (EXC 1003 - CiM), University of Münster, Germany to S.Z. N.N. is supported by the Graduate School of the Cells-in-Motion Cluster of Excellence (EXC 1003 - CiM), University of Münster, Germany.

Supplementary information

Supplementary information available online at
http://dev.biologists.org/lookup/doi/10.1242/dev.164111.supplemental

References

Ashton-Beaucage, D., Lemieux, C., Udell, C. M., Sahmi, M., Rochette, S. and Therrien, M. (2016). The deubiquitinase USP47 stabilizes MAPK by counteracting the function of the N-end rule ligase POE/UBR4 in Drosophila. *PLoS Biol.* **14**, e1002539.

Avet-Rochex, A., Kaul, A. K., Gatt, A. P., McNeill, H. and Bateman, J. M. (2012). Concerted control of gliogenesis by InR/TOR and FGF signalling in the Drosophila post-embryonic brain. *Development* **139**, 2763-2772.

Awasaki, T., Lai, S.-L., Ito, K. and Lee, T. (2008). Organization and postembryonic development of glial cells in the adult central brain of Drosophila. *J. Neurosci.* **28**, 13742-13753.

Bachmair, A., Finley, D. and Varshavsky, A. (1986). In vivo half-life of a protein is a function of its amino-terminal residue. *Science* **234**, 179-186.

Bainton, R. J., Tsai, L. T.-Y., Schwabe, T., DeSalvo, M., Gaul, U. and Heberlein, U. (2005). moody encodes two GPCRs that regulate cocaine behaviors and blood-brain barrier permeability in Drosophila. *Cell* **123**, 145-156.

Bauke, A.-C., Sasse, S., Matzat, T. and Klämbt, C. (2015). A transcriptional network controlling glial development in the Drosophila visual system. *Development* **142**, 2184-2193.

Beckervordersandforth, R. M., Rickert, C., Altenhein, B. and Technau, G. M. (2008). Subtypes of glial cells in the Drosophila embryonic ventral nerve cord as related to lineage and gene expression. *Mech. Dev.* **125**, 542-557.
Bischof, J., Maeda, R. K., Hediger, M., Karch, F. and Basler, K. (2007). An optimized transgenesis system for Drosophila using germ-line-specific phiC31 integrases. *Proc. Natl. Acad. Sci. USA* **104**, 3312-3317.
Campos-Ortega, J. A. (1997). Neurogenesis in Drosophila: an historical perspective and some prospects. *Perspect. Dev. Neurobiol.* **4**, 267-271.
Ciechanover, A. (2005). Proteolysis: from the lysosome to ubiquitin and the proteasome. *Nat. Rev. Mol. Cell Biol.* **6**, 79-87.
Cinnamon, E., Makki, R., Sawala, A., Wickenberg, L. P., Blomquist, G. J., Tittiger, C., Paroush, Z. and Gould, A. P. (2016). Drosophila Spidey/Kar regulates oenocyte growth via PI3-kinase signaling. *PLoS Genet.* **12**, e1006154.
Dantuma, N. P., Lindsten, K., Glas, R., Jellne, M. and Masucci, M. G. (2000). Short-lived green fluorescent proteins for quantifying ubiquitin/proteasome-dependent proteolysis in living cells. *Nat. Biotechnol.* **18**, 538-543.
Ditzel, M., Wilson, R., Tenev, T., Zachariou, A., Paul, A., Deas, E. and Meier, P. (2003). Degradation of DIAP1 by the N-end rule pathway is essential for regulating apoptosis. *Nat. Cell Biol.* **5**, 467-473.
Edenfeld, G., Volohonsky, G., Krukkert, K., Naffin, E., Lammel, U., Grimm, A., Engelen, D., Reuveny, A., Volk, T. and Klämbt, C. (2006). The splicing factor crooked neck associates with the RNA-binding protein HOW to control glial cell maturation in Drosophila. *Neuron* **52**, 969-980.
Edgar, B. A., Zielke, N. and Gutierrez, C. (2014). Endocycles: a recurrent evolutionary innovation for post-mitotic cell growth. *Nat. Rev. Mol. Cell Biol.* **15**, 197-210.
Eulenberg, K. G. and Schuh, R. (1997). The tracheae defective gene encodes a bZIP protein that controls tracheal cell movement during Drosophila embryogenesis. *EMBO J.* **16**, 7156-7165.
Franzdóttir, S. R., Engelen, D., Yuva-Aydemir, Y., Schmidt, I., Aho, A. and Klämbt, C. (2009). Switch in FGF signalling initiates glial differentiation in the Drosophila eye. *Nature* **460**, 758-761.
Ghosh, A., Kling, T., Snaidero, N., Sampaio, J. L., Shevchenko, A., Gras, H., Geurten, B., Göpfert, M. C., Schulz, J. B., Voigt, A. et al. (2013). A global in vivo Drosophila RNAi screen identifies a key role of ceramide phosphoethanolamine for glial ensheathment of axons. *PLoS Genet.* **9**, e1003980.
Grigoryev, S., Stewart, A. E., Kwon, Y. T., Arfin, S. M., Bradshaw, R. A., Jenkins, N. A., Copeland, N. G. and Varshavsky, A. (1996). A mouse amidase specific for N-terminal asparagine. The gene, the enzyme, and their function in the N-end rule pathway. *J. Biol. Chem.* **271**, 28521-28532.
Ito, K., Urban, J. and Technau, G. M. (1995). Distribution, classification, and development of Drosophila glial cells in the late embryonic and early larval ventral nerve cord. *Roux's Arch. Dev. Biol.* **204**, 284-307.
Kwon, Y. T., Reiss, Y., Fried, V. A., Hershko, A., Yoon, J. K., Gonda, D. K., Sangan, P., Copeland, N. G., Jenkins, N. A. and Varshavsky, A. (1998). The mouse and human genes encoding the recognition component of the N-end rule pathway. *Proc. Natl. Acad. Sci. USA* **95**, 7898-7903.
Leiserson, W. M., Harkins, E. W. and Keshishian, H. (2000). Fray, a Drosophila serine/threonine kinase homologous to mammalian PASK, is required for axonal ensheathment. *Neuron* **28**, 793-806.
Leiserson, W. M., Forbush, B. and Keshishian, H. (2011). Drosophila glia use a conserved cotransporter mechanism to regulate extracellular volume. *Glia* **59**, 320-332.
Li, D., Liu, Y., Pei, C., Zhang, P., Pan, L., Xiao, J., Meng, S., Yuan, Z. and Bi, X. (2017). miR-285-Yki/Mask double-negative feedback loop mediates blood-brain barrier integrity in Drosophila. *Proc. Natl Acad. Sci. USA* **114**, E2365-E2374.
Marshall, W. F., Young, K. D., Swaffer, M., Wood, E., Nurse, P., Kimura, A., Frankel, J., Wallingford, J., Walbot, V., Qu, X. et al. (2012). What determines cell size? *BMC Biol.* **10**, 101.
Matzat, T., Sieglitz, F., Kottmeier, R., Babatz, F., Engelen, D. and Klämbt, C. (2015). Axonal wrapping in the Drosophila PNS is controlled by glia-derived neuregulin homolog Vein. *Development* **142**, 1336-1345.
Mayer, F., Mayer, N., Chinn, L., Pinsonneault, R. L., Kroetz, D. and Bainton, R. J. (2009). Evolutionary conservation of vertebrate blood-brain barrier chemoprotective mechanisms in Drosophila. *J. Neurosci.* **29**, 3538-3550.
Meyer, H., Bug, M. and Bremer, S. (2012). Emerging functions of the VCP/p97 AAA-ATPase in the ubiquitin system. *Nat. Cell Biol.* **14**, 117-123.
Michelson, A. M., Gisselbrecht, S., Buff, E. and Skeath, J. B. (1998). Heartbroken is a specific downstream mediator of FGF receptor signalling in Drosophila. *Development* **125**, 4379-4389.
Nagarkar-Jaiswal, S., Lee, P.-T., Campbell, M. E., Chen, K., Anguiano-Zarate, S., Gutierrez, M. C., Busby, T., Lin, W.-W., He, Y., Schulze, K. L. et al. (2015). A library of MiMICs allows tagging of genes and reversible, spatial and temporal knockdown of proteins in Drosophila. *Elife* **4**, e05338.
Nern, A., Pfeiffer, B. D. and Rubin, G. M. (2015). Optimized tools for multicolor stochastic labeling reveal diverse stereotyped cell arrangements in the fly visual system. *Proc. Natl. Acad. Sci. USA* **112**, E2967-E2976.
Orr-Weaver, T. L. (2015). When bigger is better: the role of polyploidy in organogenesis. *Trends Genet.* **31**, 307-315.
Parks, A. L., Cook, K. R., Belvin, M., Dompe, N. A., Fawcett, R., Huppert, K., Tan, L. R., Winter, C. G., Bogart, K. P., Deal, J. E. et al. (2004). Systematic generation of high-resolution deletion coverage of the Drosophila melanogaster genome. *Nat. Genet.* **36**, 288-292.
Reddy, B. V. V. G. and Irvine, K. D. (2011). Regulation of Drosophila glial cell proliferation by Merlin-Hippo signaling. *Development* **138**, 5201-5212.
Reddy, B. V. V. G. and Irvine, K. D. (2013). Regulation of Hippo signaling by EGFR-MAPK signaling through Ajuba family proteins. *Dev. Cell* **24**, 459-471.
Rodrigues, F., Thuma, L. and Klämbt, C. (2012). The regulation of glial-specific splicing of Neurexin IV requires HOW and Cdk12 activity. *Development* **139**, 1765-1776.
Rumpf, S., Lee, S. B., Jan, L. Y. and Jan, Y. N. (2011). Neuronal remodeling and apoptosis require VCP-dependent degradation of the apoptosis inhibitor DIAP1. *Development* **138**, 1153-1160.
Rumpf, S., Bagley, J. A., Thompson-Peer, K. L., Zhu, S., Gorczyca, D., Beckstead, R. B., Jan, L. Y. and Jan, Y. N. (2014). Drosophila Valosin-Containing Protein is required for dendrite pruning through a regulatory role in mRNA metabolism. *Proc. Natl Acad. Sci. USA* **111**, 7331-7336.
Sasse, S. and Klämbt, C. (2016). Repulsive epithelial cues direct glial migration along the nerve. *Dev. Cell* **39**, 696-707.
Schmidt, I., Thomas, S., Kain, P., Risse, B., Naffin, E. and Klämbt, C. (2012). Kinesin heavy chain function in Drosophila glial cells controls neuronal activity. *J. Neurosci.* **32**, 7466-7476.
Schwabe, T., Bainton, R. J., Fetter, R. D., Heberlein, U. and Gaul, U. (2005). GPCR signaling is required for blood-brain barrier formation in Drosophila. *Cell* **123**, 133-144.
Sepp, K. J. and Auld, V. J. (1999). Conversion of lacZ enhancer trap lines to GAL4 lines using targeted transposition in Drosophila melanogaster. *Genetics* **151**, 1093-1101.
Sepp, K. J., Schulte, J. and Auld, V. J. (2000). Developmental dynamics of peripheral glia in Drosophila melanogaster. *Glia* **30**, 122-133.
Sieglitz, F., Matzat, T., Yuva-Adyemir, Y., Neuert, H., Altenhein, B. and Klämbt, C. (2013). Antagonistic feedback loops involving Rau and Sprouty in the Drosophila eye control neuronal and glial differentiation. *Sci. Signal.* **6**, ra96.
Silies, M., Yuva, Y., Engelen, D., Aho, A., Stork, T. and Klämbt, C. (2007). Glial cell migration in the eye disc. *J. Neurosci.* **27**, 13130-13139.
Sriram, S. M., Kim, B. Y. and Kwon, Y. T. (2011). The N-end rule pathway: emerging functions and molecular principles of substrate recognition. *Nat. Rev. Mol. Cell Biol.* **12**, 735-747.
Stork, T., Engelen, D., Krudewig, A., Silies, M., Bainton, R. J. and Klämbt, C. (2008). Organization and function of the blood-brain barrier in Drosophila. *J. Neurosci.* **28**, 587-597.
Unhavaithaya, Y. and Orr-Weaver, T. L. (2012). Polyploidization of glia in neural development links tissue growth to blood-brain barrier integrity. *Genes Dev.* **26**, 31-36.
Venken, K. J. T., Schulze, K. L., Haelterman, N. A., Pan, H., He, Y., Evans-Holm, M., Carlson, J. W., Levis, R. W., Spradling, A. C., Hoskins, R. A. et al. (2011). MiMIC: a highly versatile transposon insertion resource for engineering Drosophila melanogaster genes. *Nat. Meth.* **8**, 737-743.
Volkenhoff, A., Weiler, A., Letzel, M., Stehling, M., Klämbt, C. and Schirmeier, S. (2015). Glial glycolysis is essential for neuronal survival in Drosophila. *Cell Metab.* **22**, 437-447.
von Hilchen, C. M., Beckervordersandforth, R. M., Rickert, C., Technau, G. M. and Altenhein, B. (2008). Identity, origin, and migration of peripheral glial cells in the Drosophila embryo. *Mech. Dev.* **125**, 337-352.
von Hilchen, C. M., Bustos, Á. E., Giangrande, A., Technau, G. M. and Altenhein, B. (2013). Predetermined embryonic glial cells form the distinct glial sheaths of the Drosophila peripheral nervous system. *Development* **140**, 3657-3668.
Wójcik, C., Rowicka, M., Kudlicki, A., Nowis, D., McConnell, E., Kujawa, M. and DeMartino, G. N. (2006). Valosin-containing protein (p97) is a regulator of endoplasmic reticulum stress and of the degradation of N-end rule and ubiquitin-fusion degradation pathway substrates in mammalian cells. *Mol. Biol. Cell* **17**, 4606-4618.
Wood, E. and Nurse, P. (2015). Sizing up to divide: mitotic cell-size control in fission yeast. *Annu. Rev. Cell. Dev. Biol.* **31**, 11-29.
Xie, X. and Auld, V. J. (2011). Integrins are necessary for the development and maintenance of the glial layers in the Drosophila peripheral nerve. *Development* **138**, 3813-3822.
Xu, P., Sun, B. and Salvaterra, P. M. (1999). Organization and transcriptional regulation of Drosophila Na(+), K(+)-ATPase beta subunit genes: Nrv1 and Nrv2. *Gene* **236**, 303-313.
Yuva-Aydemir, Y., Bauke, A.-C. and Klämbt, C. (2011). Spinster controls Dpp signaling during glial migration in the Drosophila eye. *J. Neurosci.* **31**, 7005-7015.
Zhang, Y., Chen, K., Sloan, S. A., Bennett, M. L., Scholze, A. R., O'Keeffe, S., Phatnani, H. P., Guarnieri, P., Caneda, C., Ruderisch, N. et al. (2014). An RNA-sequencing transcriptome and splicing database of glia, neurons, and vascular cells of the cerebral cortex. *J. Neurosci.* **34**, 11929-11947.
Zheng, N. and Shabek, N. (2017). Ubiquitin ligases: structure, function, and regulation. *Annu. Rev. Biochem.* **86**, 129-157.
Zielke, N., Korzelius, J., van Straaten, M., Bender, K., Schuhknecht, G. F. P., Dutta, D., Xiang, J. and Edgar, B. A. (2014). Fly-FUCCI: a versatile tool for studying cell proliferation in complex tissues. *Cell Rep.* **7**, 588-598.